THE JOURNAL OF BIOLOGICAL CHEMISTRY VOL. 288, NO. 20, pp. 14125–14134, May 17, 2013

Mycobacterium smegmatis Lhr Is a DNA-dependent ATPase and a 3′-to-5′ DNA Translocase and Helicase That Prefers to Unwind 3′-Tailed RNA:DNA Hybrids*[S]

Received for publication, March 5, 2013, and in revised form, March 27, 2013 Published, JBC Papers in Press, April 2, 2013, DOI 10.1074/jbc.M113.466854

Heather Ordonez and Stewart Shuman[1]

From the Molecular Biology Program, Sloan-Kettering Institute, New York, New York 10065

Background: Helicases play important roles in nucleic acid transactions.
Results: Mycobacterial Lhr uses the energy of ATP hydrolysis to drive 3′-to-5′ translocation along single strand DNA and to unwind duplexes *en route*.
Conclusion: Lhr is better at unwinding an RNA:DNA hybrid than a DNA:DNA duplex.
Significance: Lhr defines a novel clade of helicases with a signature domain organization.

We are interested in the distinctive roster of helicases of *Mycobacterium*, a genus of the phylum Actinobacteria that includes the human pathogen *Mycobacterium tuberculosis* and its avirulent relative *Mycobacterium smegmatis*. Here, we identify and characterize *M. smegmatis* Lhr as the exemplar of a novel clade of superfamily II helicases, by virtue of its biochemical specificities and signature domain organization. Lhr is a 1507-amino acid monomeric nucleic acid-dependent ATPase that uses the energy of ATP hydrolysis to drive unidirectional 3′-to-5′ translocation along single strand DNA and to unwind duplexes *en route*. The ATPase is more active in the presence of calcium than magnesium. ATP hydrolysis is triggered by either single strand DNA or single strand RNA, yet the apparent affinity for a DNA activator is 11-fold higher than for an RNA strand of identical size and nucleobase sequence. Lhr is 8-fold better at unwinding an RNA:DNA hybrid than it is at displacing a DNA:DNA duplex of identical nucleobase sequence. The truncated derivative Lhr-(1–856) is an autonomous ATPase, 3′-to-5′ translocase, and RNA:DNA helicase. Lhr-(1–856) is 100-fold better RNA:DNA helicase than DNA:DNA helicase. Lhr homologs are found in bacteria representing eight different phyla, being especially prevalent in Actinobacteria (including *M. tuberculosis*) and Proteobacteria (including *Escherichia coli*).

DNA helicases are nucleic acid-dependent NTPases that play important roles in DNA replication, recombination, and repair. RNA helicases orchestrate transcription, RNA processing, ribosome biogenesis, translation, and RNA turnover. Helicases use the chemical energy of NTP hydrolysis to either effect mechanical changes in the secondary structure of nucleic acids or to remodel the structures of protein-nucleic acid complexes. Helicases have been classified into superfamilies, families, and subfamilies according to their distinctive primary, tertiary, and quaternary structures and their biochemical specificities: *i.e.* their NTP preference, nucleic acid preference, and directionality of translocation or unwinding (1).

Differences in the roster of DNA helicases between taxa offer useful clues to the evolution and diversification of replication/repair strategies and, where the rosters diverge in animals *versus* infectious pathogens, they can suggest anti-infective drug targets. With this in mind, we are focused on the ensemble of DNA helicases in *Mycobacterium*, a genus of the phylum Actinobacteria that includes the human pathogen *Mycobacterium tuberculosis* and its avirulent relative *Mycobacterium smegmatis*. To date, seven mycobacterial DNA helicases have been purified and characterized: UvrD1, UvrD2, and AdnAB are superfamily I helicases; XBP, RqlH, SftH, and RecG are superfamily II (SF2)[2] helicases. UvrD1 (2–6), UvrD2 (2, 7, 8), XBP (9–11), RqlH (12), and SftH (13) are monomeric proteins that unwind 3′-tailed duplex DNAs by loading onto the 3′ single strand and translocating in the 3′-to-5′ direction. RecG unwinds multi-strand DNA junctions that resemble stalled replication forks or recombination intermediates (14). AdnAB is a heterodimeric motor nuclease machine that unwinds and resects DNA double strand breaks during homologous recombination (15–18). The 3′-to-5′ translocase-helicase activity of the AdnB subunit drives unwinding from a duplex end, during which the AdnA and AdnB nucleases incise the displaced 5′ and 3′ strands, respectively. Of the seven biochemically characterized helicases, only UvrD2 has been shown to be essential for mycobacterial growth in culture (7, 8).

Here, we identify, purify, and biochemically characterize a new mycobacterial SF2 helicase named Lhr, in deference to its extensive homology to the Lhr polypeptide of *Escherichia coli*. The *E. coli lhr* gene (long helicase-related) was originally identified and studied by Deutscher and co-workers (19) because of its location immediately downstream of the *rnt* gene encoding the tRNA-processing enzyme RNase T. The 1538-aa Lhr polypeptide was, at the time, the longest known *E. coli* protein; it is presently the fifth largest *E. coli* protein after YeeJ (2358-aa), YdbA' (2020-aa), YneoO' (1806-aa) and YfhM (1653-aa).

* This work was supported by National Institutes of Health Grant AI64693.
[S] This article contains supplemental Table S1 and Fig. S1.
[1] An American Cancer Society Research Professor. To whom correspondence should be addressed. E-mail: shuman@ski.mskcc.org.

[2] The abbreviations used are: SF2, superfamily II; SA, streptavidin; aa, amino acid(s).

Although *E. coli* Lhr was predicted to be an SF2 helicase, Reuven *et al.* (19) were unable to demonstrate any nucleic-acid-dependent ATPase activity associated with this protein. Disruption of the *E. coli lhr* gene by insertion of a kanamycin-resistance cassette near the 5′ end of the ORF (which interrupts the putative motor domain) had no effect on *E. coli* growth under a wide variety of conditions tested (19). The *lhr*::*kan* mutation did not sensitize *E. coli* to killing by UV or peroxide, and there was no synthetic growth phenotype when *lhr*::*kan* was combined with *recA*, *recB*, *recD*, *uvrD*, *uvrB*, *uvrD*, or *rep* (19).

The 1507-aa *M. smegmatis* Lhr protein and the corresponding 1513-aa *M. tuberculosis* Lhr protein are encoded by genes Msmeg_1757 and Rv3296, respectively. The N-terminal third of mycobacterial Lhr resembles the NTPase domains of SF2 helicases, as defined by the following characteristic motifs (highlighted in Fig. 1): (i) motif I GxGKT (the P-loop or Walker A-box), the lysine side chain of which contacts the β and γ phosphates of the NTP substrate and the serine of which coordinates the metal cofactor; (ii) motif II DExH (the Walker B-box), which coordinates the metal cofactor; (iii) motif VI QxxGRxGH, which coordinates the NTP γ phosphate and the water nucleophile for NTP hydrolysis; and (iv) motif III SAT, which makes bridging contacts to motifs II and VI and couples NTP hydrolysis to motor activity (20, 21). The C-terminal two-thirds of Lhr has no instructive motifs or homologies to any proteins outside the clade of Lhr homologs found in many diverse bacterial taxa (Table S1). To the extent that the genetic neighbor might suggest biological function, it is worth noting that the *nei* gene immediately downstream of *lhr* in *M. smegmatis* and *M. tuberculosis* encodes the DNA repair enzyme endonuclease VIII (22).

To our knowledge, there has been no prior characterization of any bacterial Lhr enzyme. To fill this knowledge gap, we produced, purified, and characterized recombinant *M. smegmatis* Lhr. Key points of interest for this study were as follows. (i) Is Lhr a nucleic acid-dependent phosphohydrolase and, if so, what is its substrate and cofactor specificity? (ii) Can Lhr couple NTP hydrolysis to mechanical work, especially duplex unwinding? (iii) Do the biochemical activities of Lhr point to a role in DNA or RNA transactions? (iv) Is the C-terminal domain of Lhr required for its activities?

EXPERIMENTAL PROCEDURES

Lhr Proteins—The ORFs encoding full-length *M. smegmatis* Lhr (Msmeg_1757) and C-terminal truncations Lhr-(1–562), Lhr-(1–856), and Lhr-(1–1098) were PCR-amplified from *M. smegmatis* genomic DNA with primers that introduced a NdeI site at the start codon and a XhoI site downstream of the native or newly installed stop codons. The PCR products were digested with NdeI and XhoI and ligated into pET16b that had been digested with NdeI and XhoI. The resulting pET-Lhr plasmids encode His_{10}-tagged Lhr polypeptides under the transcriptional control of a T7 RNA polymerase promoter. The plasmid inserts were sequenced to verify that no unintended coding changes were acquired during amplification and cloning. The pET16b-Lhr plasmids were transformed into *E. coli* BL21(DE3) cells. Cultures (1-liter) amplified from single ampicillin-resistant transformants were grown at 37 °C in LB broth

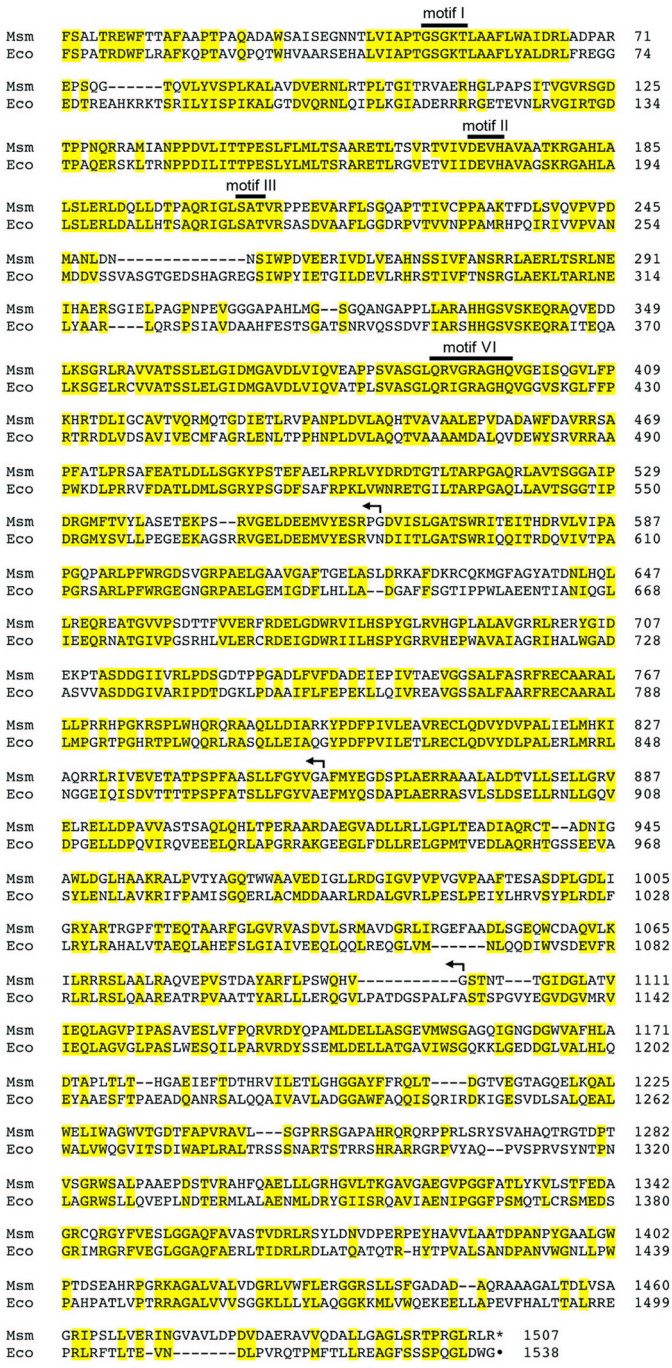

FIGURE 1. **Primary structure of *M. smegmatis* Lhr.** The amino acid sequence of the 1507-aa *M. smegmatis* (*Msm*) Lhr polypeptide is aligned to that of the homologous *E. coli* (*Eco*) Lhr protein. Positions of side chain identity/similarity are highlighted in *yellow*. Gaps in the alignments are denoted by *dashes*. The SF2 NTPase motifs I, II, III, and VI are labeled and highlighted by bars *above* the sequences. The C-terminal margins in the Lhr-(1–562), Lhr-(1–856), and Lhr-(1–1098) truncations are denoted by *arrows*.

containing 100 μg/ml ampicillin until the A_{600} reached 0.5. The cultures were chilled on ice for 1 h and then adjusted to 2% (v/v) ethanol and 0.3 mM isopropyl-β-D-thiogalactopyranoside and incubated for 16 h at 17 °C with constant shaking. All subsequent procedures were performed at 4 °C. Cells were harvested by centrifugation and resuspended in 25 ml of buffer A (50 mM Tris-HCl, pH 8.0, 500 mM NaCl, 1 mM DTT, 10% sucrose) containing 1 protease inhibitor mixture tablet (Roche Diagnostics).

Lysozyme was added to a concentration of 1 mg/ml, and the suspension was incubated for 30 min before adding Triton X-100 to a final concentration of 0.1%. After incubation for an additional 30 min, the lysate was sonicated to reduce viscosity, and the insoluble material was pelleted by centrifugation at 38,000 × *g* for 1 h. The supernatant was mixed for 1 h with 2 ml of nickel-nitrilotriacetic acid-agarose resin (Qiagen) that had been equilibrated with buffer A. The resin was recovered by centrifugation and resuspended in 30 ml of buffer A. The resin was again recovered by centrifugation and then resuspended in 10 ml of buffer B (50 mM Tris-HCl, pH 8.0, 500 mM NaCl, 0.05% Triton X-100, 10% glycerol) containing 50 mM imidazole and poured into a column. After washing the column with 4 ml of 3 M KCl, the bound material was eluted stepwise with 4-ml aliquots of 50, 100, and 500 mM imidazole in buffer B. The polypeptide compositions of the eluate fractions were monitored by SDS-PAGE. The recombinant Lhr proteins were recovered in the 100 and 500 mM imidazole fractions, which were pooled and then dialyzed overnight against 4 liters of buffer C (50 mM Tris-HCl, pH 8.0, 500 mM NaCl, 1 mM DTT, 1 mM EDTA, 0.05% Triton X-100, 10% glycerol). To deplete residual nucleic acids, the dialyzed Lhr preparations were applied to 2-ml DEAE-Sephacel columns that had been equilibrated with buffer C, and the Lhr proteins were recovered in the flow-through fraction. Total protein concentrations of the DEAE preparations were gauged with the Bio-Rad dye reagent using BSA as the standard. The concentrations of the full-length Lhr and truncated Lhr-(1–562), Lhr-(1–856), and Lhr-(1–1098) polypeptides were then determined by SDS-PAGE analysis of aliquots of each preparation (5 μg) in parallel with 1.25, 2.5, 5, and 10 μg of a BSA standard. The gel was stained with Coomassie Blue, and the staining intensities of the Lhr and BSA polypeptides were quantified using a Chemidoc XRS imager and Quantity One software. Lhr concentrations were calculated by interpolating the staining intensities to the BSA standard curve. The yields of Lhr and Lhr truncations were ~25 mg per liter of culture.

Nucleoside Triphosphatase Assay—Reaction mixtures containing (per 10 μl) 20 mM Tris-HCl, pH 7.0, 1 mM DTT, 1 mM $CaCl_2$, 1 mM [α-^{32}P]ATP (Perkin-Elmer Life Sciences), and DNA and Lhr as specified were incubated for 30 min at 37 °C. The reactions were quenched by adding 2 μl of 5 M formic acid. An aliquot (2 μl) of the mixture was applied to a polyethyleneimine-cellulose TLC plate, which was developed with 0.45 M ammonium sulfate. The radiolabeled material was visualized by autoradiography and [^{32}P]ADP formation was quantified by scanning the TLC plate with a Fujix BAS2500 imager.

Streptavidin Displacement Assay of Lhr Translocation on DNA—Synthetic 34-mer oligodeoxynucleotides of otherwise identical nucleobase sequence containing a biotin-ON internucleotide spacer either at the fourth position from the 5′ terminus or the second position from the 3′ terminus were purchased from Eurofins MWG Operon. These DNAs were 5′ end-labeled with [γ-^{32}P]ATP by using T4 polynucleotide kinase and then purified by electrophoresis through a native 18% polyacrylamide gel. Streptavidin-DNA (SA-DNA) complexes were formed by preincubating 100 nM biotinylated [^{32}P]DNA with 4 μM streptavidin (Sigma) in 20 mM Tris-HCl, pH 7.0, 1 mM DTT, 1 mM $CaCl_2$, and 1 mM ATP for 15 min at room temperature. The mixtures were supplemented with 40 μM free biotin (Fisher) and the displacement reactions (10 μl, containing 1 pmol biotinylated [^{32}P]DNA) were initiated by adding 10 pmol of Lhr. After incubation for 15 min at 37 °C, the reactions were quenched by adding 3 μl of a solution containing 200 mM EDTA, 0.6% SDS, 25% glycerol, and 20 μM of an unlabeled single strand DNA to mask any binding of Lhr to [^{32}P]DNA released from the SA-DNA complex. The reaction products were analyzed by electrophoresis through a 15-cm native 15% polyacrylamide gel containing 89 mM Tris borate, 2.5 mM EDTA. The free ^{32}P-labeled 34-mer DNA and the SA-DNA complexes were visualized by autoradiography.

Helicase Assay—The 5′ ^{32}P-labeled DNA strand was prepared by reaction of a synthetic oligodeoxynucleotide with T4 polynucleotide kinase and [γ-^{32}P]ATP. The labeled DNA was separated from ATP by gel filtration through a G-50 micro column (GE Healthcare) and then annealed to a 3-fold excess of a complementary DNA strand to form the various substrates shown in the figures. The annealed DNAs were purified by electrophoresis through a native 12% polyacrylamide gel, eluted from an excised gel slice by incubation for 16 h at 4 °C in 200 μl 10 mM Tris-HCl, pH 7.5, 1 mM EDTA, recovered by ethanol precipitation and resuspended in water. The 5′ ^{32}P-labeled RNA strand was prepared by reaction of a synthetic oligonucleotide with T4 polynucleotide kinase and [γ-^{32}P]ATP. The labeled RNA was separated from ATP by electrophoresis through a 40-cm 15% polyacrylamide gel containing 7 M urea in 89 mM Tris borate, 2.5 mM EDTA. The RNA was eluted from an excised gel slice by incubation for 16 h at 4 °C in 1 M ammonium acetate, 0.2% SDS, 20 mM EDTA. The RNA was recovered by ethanol precipitation and resuspended in 10 mM Tris-HCl, pH 6.8, 1 mM EDTA. Annealing of the labeled RNA to complementary strands and gel purification of the duplexes was performed as described above for the labeled DNA duplexes. Helicase reaction mixtures (10 μl) containing 20 mM Tris-HCl, pH 7.0, 1 mM DTT, 5 mM $CaCl_2$, ^{32}P-labeled nucleic acid as specified, and Lhr as specified were preincubated for 10 min at room temperature. The reactions were initiated by adding 1 mM ATP and a 10-fold excess of an unlabeled oligonucleotide identical to the labeled strand of the helicase substrate. Addition of excess unlabeled strand was necessary to prevent the spontaneous reannealing of the unwound ^{32}P-labeled strand. The reaction mixtures were incubated for 30 min at 37 °C and then quenched by adding 1 μl of a solution containing 5% SDS, 100 mM EDTA. The mixtures were supplemented with 4 μl of 50% glycerol, 0.3% bromphenol blue. The reaction products were analyzed by electrophoresis through a 15-cm 12% polyacrylamide gel in 89 mM Tris borate, 2.5 mM EDTA. The products were visualized by autoradiography.

RESULTS

Recombinant Lhr Is a Monomeric DNA-dependent ATPase—To evaluate the enzymatic and physical properties of *M. smegmatis* Lhr, we produced the full-length 1507-aa protein in *E. coli* as a His_{10} fusion and purified it from a soluble extract by nickel-agarose and DEAE-Sephacel chromatography (Fig. 2*A*, WT). We also produced and purified three C-terminal truncation mutants: Lhr-(1–1098), Lhr-(1–856), and Lhr-(1–562),

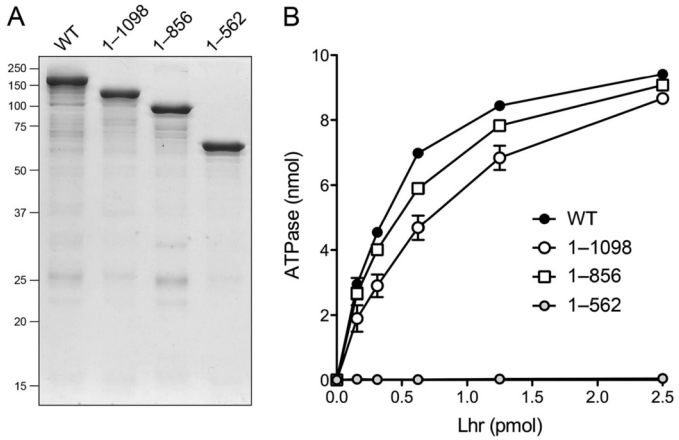

FIGURE 2. **Lhr is an ATP phosphohydrolase.** *A*, purification. Aliquots (5 μg) of full-length Lhr and truncated proteins Lhr-(1–1098), Lhr-(1–856), and Lhr-(1–562) were analyzed by SDS-PAGE. The Coomassie Blue-stained gel is shown. The positions and sizes (kDa) of marker polypeptides are indicated on the *left*. *B*, ATPase reaction mixtures (10 μl) containing 20 mM Tris-HCl, pH 7.0, 1 mM DTT, 1 mM $CaCl_2$, 1 mM [α-^{32}P]ATP (10 nmol of ATP), 5 μM 80-mer single strand DNA oligonucleotide, and Lhr proteins as specified were incubated at 37 °C for 30 min. The reaction products were analyzed by TLC. The extents of [^{32}P]ADP formation are plotted as a function of input Lhr. Data are the average of three separate enzyme titration experiments ± S.E.

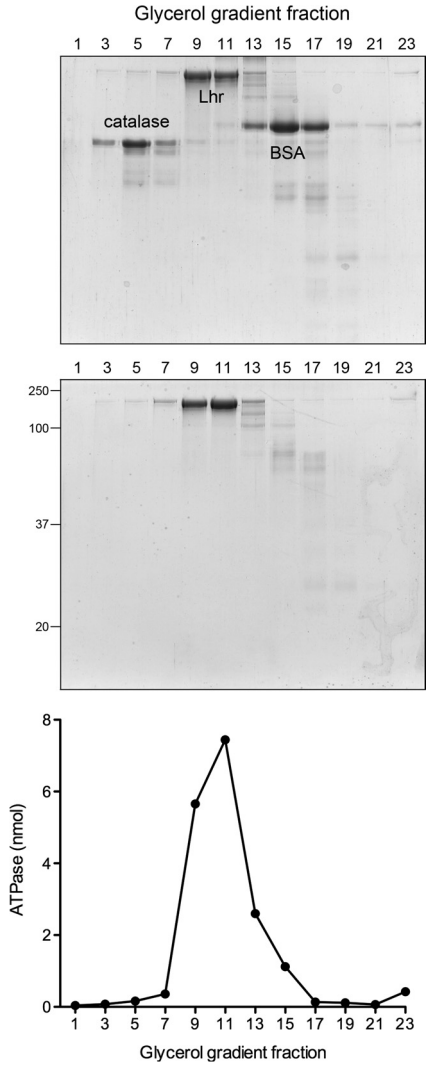

FIGURE 3. **Glycerol gradient sedimentation.** Aliquots of Lhr (200 μg in 0.2 ml), either alone (*middle panel*) or mixed with 50 μg of catalase and 50 μg of BSA (*top panel*) were applied to 4.8-ml 15–30% glycerol gradients containing 50 mM Tris-HCl, pH 8.0, 500 mM NaCl, 1 mM DTT, 1 mM EDTA, and 0.05% Triton X-100. The gradients were centrifuged at 50,000 rpm for 17 h at 4 °C in a Beckman SW55Ti rotor. Fractions (0.2 ml) were collected from the bottoms of the tubes. Aliquots (20 μl) of the odd-numbered fractions (fraction 1 being at the bottom of the gradient) were analyzed by SDS-PAGE. The Coomassie Blue-stained gels are shown. The Lhr, catalase, and BSA polypeptide are labeled. Aliquots (1 μl) of the odd-numbered fractions from the Lhr-only gradient were assayed for ATPase activity in reaction mixtures (10 μl) containing 20 mM Tris-HCl, pH 7.0, 1 mM DTT, 1 mM $CaCl_2$, 1 mM [α-^{32}P]ATP, and 5 μM 80-mer DNA oligonucleotide. The activity profile is plotted.

which displayed the expected serial decrements in apparent molecular weight when analyzed by SDS-PAGE (Fig. 2*A*). Reaction of wild-type Lhr with 1 mM [α-^{32}P]ATP in the presence of calcium and single strand DNA resulted in the hydrolysis of [α-^{32}P]ATP to [α-^{32}P]ADP, as monitored by polyethyleneimine-cellulose TLC. The extent of ATP hydrolysis was proportional to input Lhr and >90% of the ATP was hydrolyzed at saturating enzyme (Fig. 2*B*). No conversion of [α-^{32}P]ADP to [^{32}P]AMP was detected. Whereas the Lhr-(1–1098) and Lhr-(1–856) variants displayed similar ATPase specific activity to that of the wild-type Lhr, the Lhr-(1–562) variant was catalytically inert (Fig. 2*B*). We conclude that (i) the C-terminal 651 amino acids are dispensable for ATP phosphohydrolase activity; and (ii) the segment from aa 563 to 856 includes structural elements required for DNA-dependent ATP hydrolysis.

The native size of full-length Lhr was analyzed by zonal velocity sedimentation through a 15–30% glycerol gradient. The Lhr preparation was sedimented alone and, in a parallel gradient, as a mixture with marker proteins catalase and BSA. SDS-PAGE analysis of the odd-numbered fractions of the "Lhr alone" glycerol gradient revealed that the Lhr polypeptide (calculated 165 kDa) sedimented as a single component peaking in fractions 9–11 (Fig. 3, *middle panel*). Note that the minor lower molecular weight contaminant polypeptides seen in the DEAE-Sephacel Lhr preparation (Fig. 2*A*) were separated from intact Lhr during the sedimentation procedure and were recovered in the "lighter" gradient fractions 13 to 19 (Fig. 3, *middle panel*). Aliquots of the odd numbered gradient fractions were incubated with 1 mM [α-^{32}P]ATP in the presence of calcium and single strand DNA and the hydrolysis of [α-^{32}P]ATP to [α-^{32}P]ADP was monitored by TLC. The ATPase activity profile paralleled the abundance of the Lhr protein, peaking in fractions 9 to 11 (Fig. 3, *bottom panel*). These results indicate that the DNA-dependent ATPase activity is inherent to Lhr.

SDS-PAGE analysis of the odd-numbered fractions of the "Lhr plus markers" glycerol gradient (Fig. 3, *top panel*) showed that Lhr again sedimented as a discrete peak (fractions 9–11) midway between catalase (peak fraction 5; native size, 250 kDa) and BSA (peak fraction 15, native size, 66 kDa). We surmise that Lhr is a monomer in solution.

Requirements for the Lhr ATPase Activity—The ATPase activity of Lhr in the presence of an 80-mer single strand DNA required a divalent cation cofactor (Fig. 4*A*). When various metals were tested at 1 mM concentration, the divalent cation requirement for ATP hydrolysis was satisfied best by calcium (Fig. 4*A*). Magnesium and manganese were 40% as effective as calcium; nickel and zinc were 6–9% as effective. Copper and

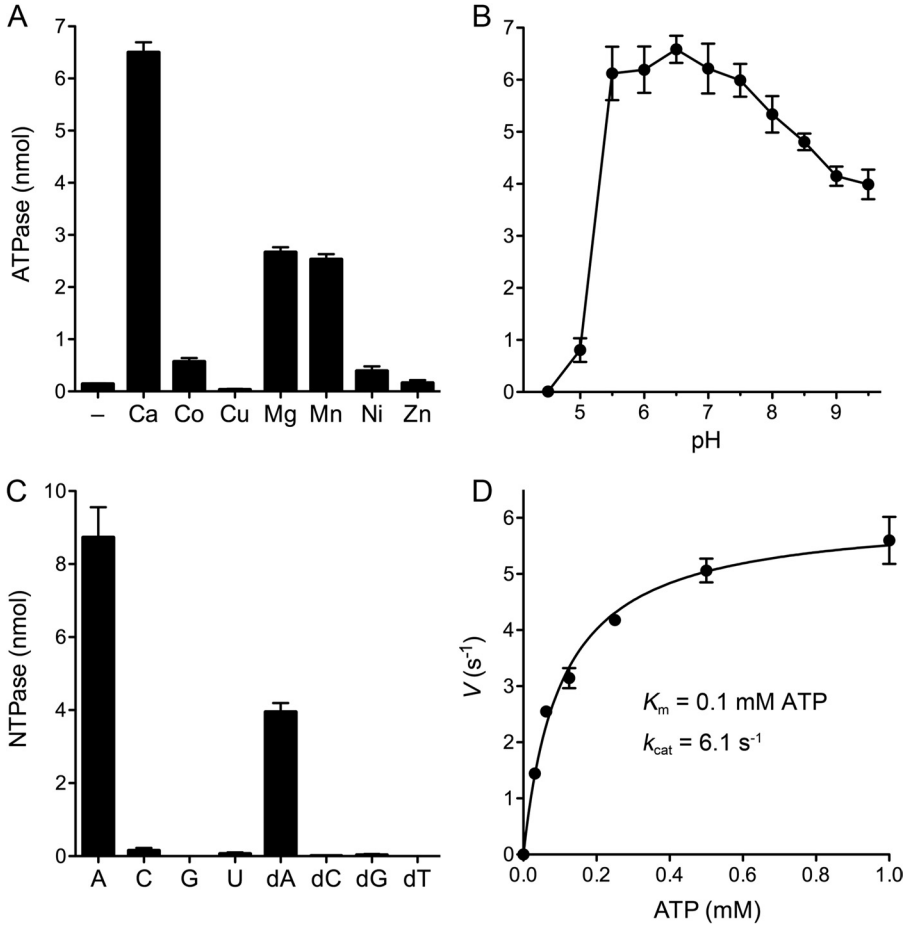

FIGURE 4. **Characterization of the Lhr NTP phosphohydrolase activity.** *A*, divalent cation specificity. Reaction mixtures (10 μl) containing 20 mM Tris-HCl, pH 7.0, 1 mM [α-^{32}P]ATP, 5 μM 80-mer DNA, 50 nM Lhr, and 1 mM of the indicated divalent cation (chloride salt) were incubated at 37 °C for 30 min. The extents of ATP hydrolysis are plotted. Data are the average of three separate experiments ± S.E. *B*. pH profile. Reaction mixtures (10 μl) containing 20 mM Tris buffer (Tris acetate, pH 4.5, 5.0, 5.5, 6.0, or 6.5 or Tris-HCl, pH 7.0, 7.5, 8.0, 8.5, 9.0, or 9.5), 1 mM DTT, 1 mM $CaCl_2$, 1 mM [α-^{32}P]ATP, 5 μM 80-mer DNA, and 50 nM Lhr were incubated at 37 °C for 30 min. The extents of ATP hydrolysis are plotted as a function of pH. Data are the average of three separate experiments ± S.E. *C*, NTP specificity. Reaction mixtures (10 μl) containing 20 mM Tris-HCl, pH 7.0, 1 mM DTT, 1 mM $CaCl_2$, 5 μM 80-mer DNA, 100 nM Lhr, and 1 mM of the indicated NTP or dNTP were incubated at 37 °C for 30 min. The reactions were quenched with 990 μl of malachite green reagent (Biomol Research Laboratories). Phosphate release was quantified by measuring A_{620} and interpolating the value to a phosphate standard curve. The values were corrected for the low levels of phosphate measured in control reaction mixtures containing 1 mM of the indicated NTP/dNTP but no added enzyme. Data are the average of three separate experiments ± S.E. *D*, steady-state kinetics. Reaction mixtures (40 μl) containing 20 mM Tris-HCl, pH 7.0, 1 mM DTT, 1 mM $CaCl_2$, 5 μM 80-mer DNA, 200 nM Lhr, and either 0.0625, 0.125, 0.25, 0.5, or 1.0 mM [α-^{32}P]ATP were incubated at 37 °C. Aliquots (10 μl) were withdrawn at 10 and 20 s (for 0.0625, 0.125, 0.25, 0.5 mM ATP), or 15 and 30 s (for 1.0 mM ATP), and quenched immediately with formic acid. The extents of ATP hydrolysis were plotted as a function of time for each ATP concentration, and the initial rates were derived by linear regression analysis in Prism. The initial rates (pmol·s^{-1}) were divided by the molar amount of input enzyme to obtain a turnover number V (s^{-1}), which is plotted in the figure as a function of ATP concentration. Data are the average of three separate experiments ± S.E. A nonlinear regression curve fit of the data to the Michaelis-Menten equation (in Prism) is shown. The K_m and k_{cat} values are indicated.

zinc were ineffective (Fig. 4*A*). Calcium and magnesium titration experiments showed that hydrolysis of 1 mM ATP was optimal at 0.5 to 1 mM (data not shown). ATP hydrolysis in the presence of calcium and 80-mer DNA was optimal from pH 5.5 to 7.5 in Tris buffer; activity declined sharply at pH 5.0 and was nil at pH 4.5 (Fig. 4*B*). Activity declined gradually at alkaline pH, to 60% of the peak value at pH 9.5 (Fig. 4*B*).

NTP Substrate Specificity—NTP substrate specificity was examined by colorimetric assay of the release of P_i from unlabeled ribonucleotides ATP, GTP, CTP, or UTP and deoxynucleotides dATP, dGTP, dCTP, or dTTP, each at 1 mM concentration. Lhr specifically hydrolyzed ATP and dATP; the other rNTPs and dNTPs were ineffective as substrates (Fig. 4*C*).

Steady-state Kinetics of ATP Hydrolysis—We determined steady-state kinetic parameters by measuring the velocity of ATP hydrolysis as a function of ATP concentration in the presence of 1 mM calcium and 5 μM 80-mer single strand DNA cofactor (Fig. 4*D*). From a nonlinear regression curve fit of the data to the Michaelis-Menten equation, we calculated that Lhr has a K_m of 0.10 ± 0.01 mM ATP and a k_{cat} of 6.1 ± 0.2 s^{-1}.

Lhr Translocates Unidirectionally 3′-to-5′ on Single Strand DNA—NTP hydrolysis by nucleic acid-dependent phosphohydrolases is often coupled to mechanical work, either duplex unwinding or displacement of protein-nucleic acid complexes, as a consequence of translocation of the phosphohydrolase enzyme along the nucleic acid. To address whether Lhr has translocase activity, we employed a streptavidin displacement assay (12, 13, 16, 23–25) as follows. ^{32}P-Labeled 34-mer DNA oligonucleotides containing a single biotin moiety at the fourth internucleotide from the 5′ end or the second internucleotide from the 3′ end were preincubated with excess SA to form a stable SA-DNA complex that was easily resolved from free

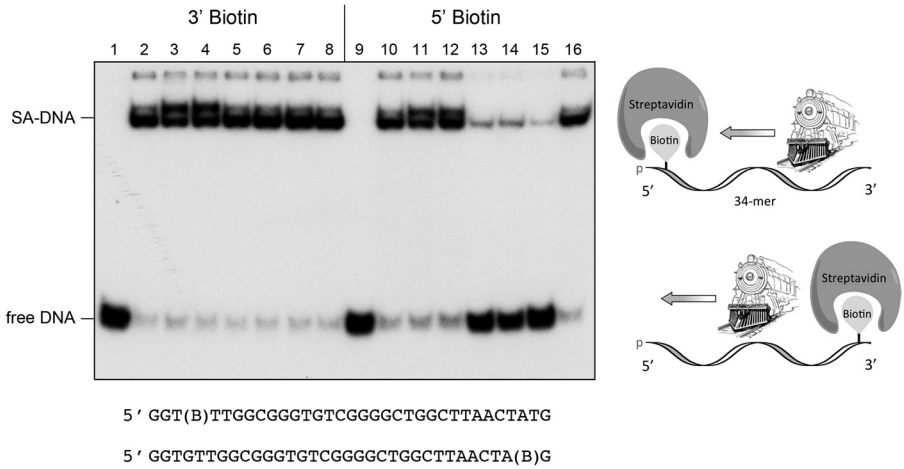

FIGURE 5. **Lhr translocates 3′-to-5′ on single-stranded DNA.** A schematic representation of the Lhr translocase motor as a cowcatcher that pries apart the otherwise stable streptavidin-biotin complex at the 5′ end of the single strand 34-mer DNA is shown on the *right*. Translocase assays were performed as described under "Experimental Procedures." Native PAGE analysis of the translocase reaction products is shown on the *left*. The species corresponding to SA-DNA complex and free DNA are indicated. The nucleobase sequences of the 5′ ^{32}P-labeled 5′- or 3′-biotinylated 34-mer single strand DNAs are shown at the *bottom* with *B* signifying the position of the biotin spacer. The complete translocase reaction mixtures in *lanes 5–8* and *13–16* contained 1 mM ATP, 1 mM $CaCl_2$, 100 nM ^{32}P-labeled 3′, or 5′-biotinylated DNA bound to streptavidin, and 1 μM Lhr (*lanes 5* and *13*), Lhr-(1–1098) (*lanes 6* and *14*), Lhr-(1–856) (*lanes 7* and *15*), or Lhr-(1–562) (*lanes 8* and *16*). Enzyme was omitted from control reactions in *lanes 2* and *10*. Enzyme and streptavidin were both omitted from control reactions in *lanes 1* and *9*. ATP was omitted from the reactions in *lanes 3* and *11*. Calcium was omitted and 5 mM EDTA was added to the reactions in *lanes 4* and *12*.

biotinylated 34-mer DNA during native PAGE (Fig. 5). The translocation assay scores the motor-dependent displacement of SA from the DNA in the presence of ATP and excess free biotin, which instantly binds to free SA and precludes SA rebinding to the labeled DNA. The rationale of the assay is that directional tracking of the motor along the DNA single strand will displace SA from one DNA end, but not the other end. When moving 3′ to 5′, it can displace SA as it collides with the 5′ biotin-SA. In contrast, a 3′ biotin-SA is not expected to be displaced by a 3′-to-5′ translocase because the protein moves away from the SA and simply falls off the free 5′ end (Fig. 5). The converse outcomes apply to a 5′-to-3′ translocase; it displaces a 3′ SA, but not a 5′ SA. The instructive finding was that Lhr displaced SA from a 5′ biotin-SA complex on the 34-mer single strand DNA to yield the free ^{32}P-labeled 34-mer strand (Fig. 5, *lane 13*) but was unable to displace SA from a 3′ biotin-SA complex tested in parallel (Fig. 5, *lane 5*). Stripping of the 5′ biotin-SA complex by Lhr to liberate free DNA depended on ATP and calcium (Fig. 5, *lanes 11* and *12*). Another instructive finding was that the ATPase-proficient truncated proteins Lhr-(1–1098) and Lhr-(1–856) were active as 3′-to-5′ translocases (Fig. 5, *lanes 14* and *15*), whereas the ATPase-defective Lhr-(1–562) was not (Fig. 5, *lane 16*). Control experiments showed that the capacity of the 5′ and 3′ biotin-modified DNA strands to activate ATP hydrolysis by Lhr was not impeded by the inclusion of excess SA in the reaction mixtures (supplemental Fig. S1). We surmise from this result that a 3′ biotin-SA complex does not inhibit the loading of Lhr on the DNA strand, fortifying our inference from the SA displacement experiments that Lhr translocates 3′-to-5′ but not 5′-to-3′.

Lhr Is a 3′-to-5′ DNA Helicase—In light of the 3′-to-5′ translocase activity demonstrated above, we tested Lhr for helicase activity with a 3′-tailed duplex substrate consisting of a 31-bp duplex with a 28-nt 3′ single strand tail to serve as a potential "loading strand" (Fig. 6). The helicase assay format we used entailed preincubation of Lhr and labeled DNA, followed by initiation of unwinding by addition of ATP, with simultaneous addition of a "trap" of excess unlabeled 59-mer displaced strand that (i) minimizes reannealing of any ^{32}P-labeled 59-mer that was unwound by Lhr and (ii) competes with the loading strand for binding to any free Lhr or Lhr that dissociated from the labeled DNA without unwinding it. Consequently, the assay predominantly gauges a single round of strand displacement by Lhr bound to the labeled 3′-tailed duplex prior to the onset of ATP hydrolysis. We found that Lhr unwound the 3′-tailed DNA substrates to yield a radiolabeled free single strand that migrated faster than the input tailed duplex during native PAGE (Fig. 6*A*); the helicase reaction product comigrated with free 59-mer generated by thermal denaturation of the substrate (Fig. 6*A*, *lane* Δ). Lhr failed to unwind a 59-bp blunt duplex DNA substrate (Fig. 6), thereby attesting to a requirement for a single strand tail to serve as a loading strand for the helicase. Lhr also failed to unwind a 5′-tailed duplex substrate (Fig. 6*A*). Lhr did unwind a "Y fork" duplex consisting of a 31-bp duplex with one blunt end and 28-nt 5′ and 3′ single strand tails at the other end (Fig. 6*A*). Assaying the Lhr glycerol gradient fractions for DNA unwinding verified that the helicase activity cosedimented with Lhr in fractions 9–11 (Fig. 6*B*). These results establish that Lhr is a unidirectional motor, powered by ATP hydrolysis, which tracks 3′-to-5′ along the loading strand and unwinds duplex DNA.

Single Strand DNA Length Requirement for ATP Hydrolysis—We tested the ability of single strand DNAs of varying length to activate ATP hydrolysis by Lhr. Titration of the oligonucleotides revealed a hyperbolic dependence of ATP hydrolysis on the amount of 59-mer, 24-mer, 18-mer, or 12-mer strands (Fig. 7*A*). Nonlinear regression fitting of the data to a one-site binding model in Prism yielded apparent K_d values as follows: 9.4 ± 0.9 nM 59-mer; 11 ± 1.5 nM 24-mer; 27 ± 2.6 nM 18-mer; and 210 ± 45 nM 12-mer. By contrast, a 6-mer oligonucleotide was ineffective at up to 2 μM concentration (Fig. 7*A*).

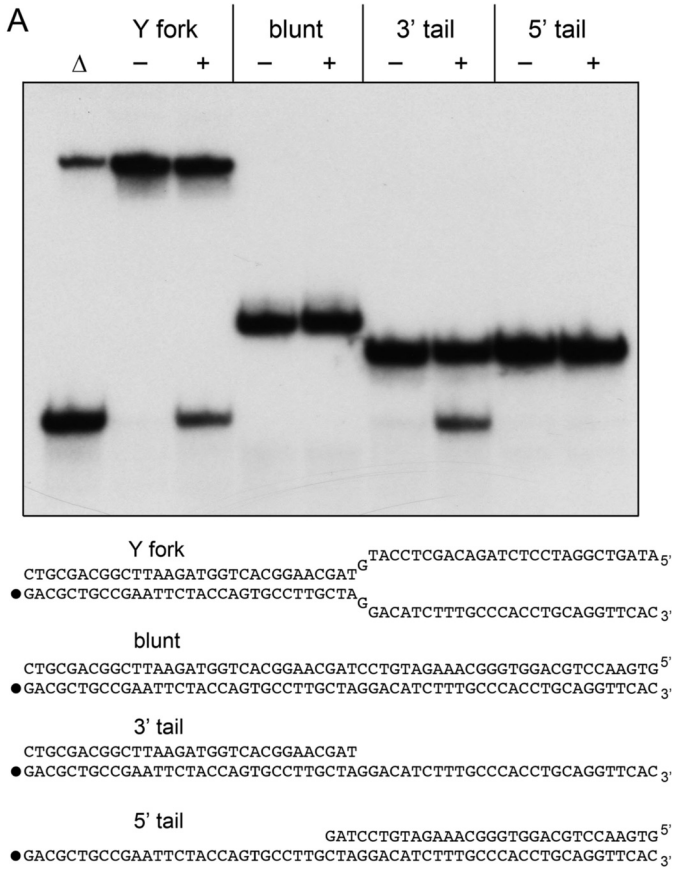

FIGURE 6. **Lhr is a 3′-to-5′ DNA helicase.** *A*, helicase reaction mixtures (10 μl) contained 20 mM Tris-HCl, pH 7.0, 1 mM DTT, 5 mM $CaCl_2$, 100 nM of the indicated DNA substrate (depicted at the *bottom*, with the 5′ ^{32}P label denoted by ●), 1 mM ATP, and 1 μM Lhr (indicated by +). Lhr was omitted from the reaction mixtures in lanes (−). A reaction mixture lacking Lhr that was heat-denatured prior to PAGE is included in *lane* Δ. The reaction products were analyzed by native PAGE and visualized by autoradiography. *B*, helicase reaction mixtures (10 μl) contained 20 mM Tris-HCl, pH 7.0, 1 mM DTT, 5 mM $CaCl_2$, 100 nM 5′ ^{32}P-labeled 3′-tailed duplex DNA substrate (as in *A*), 1 mM ATP, and 1 μl of the indicated glycerol gradient fractions. The products were analyzed by native PAGE and visualized by autoradiography.

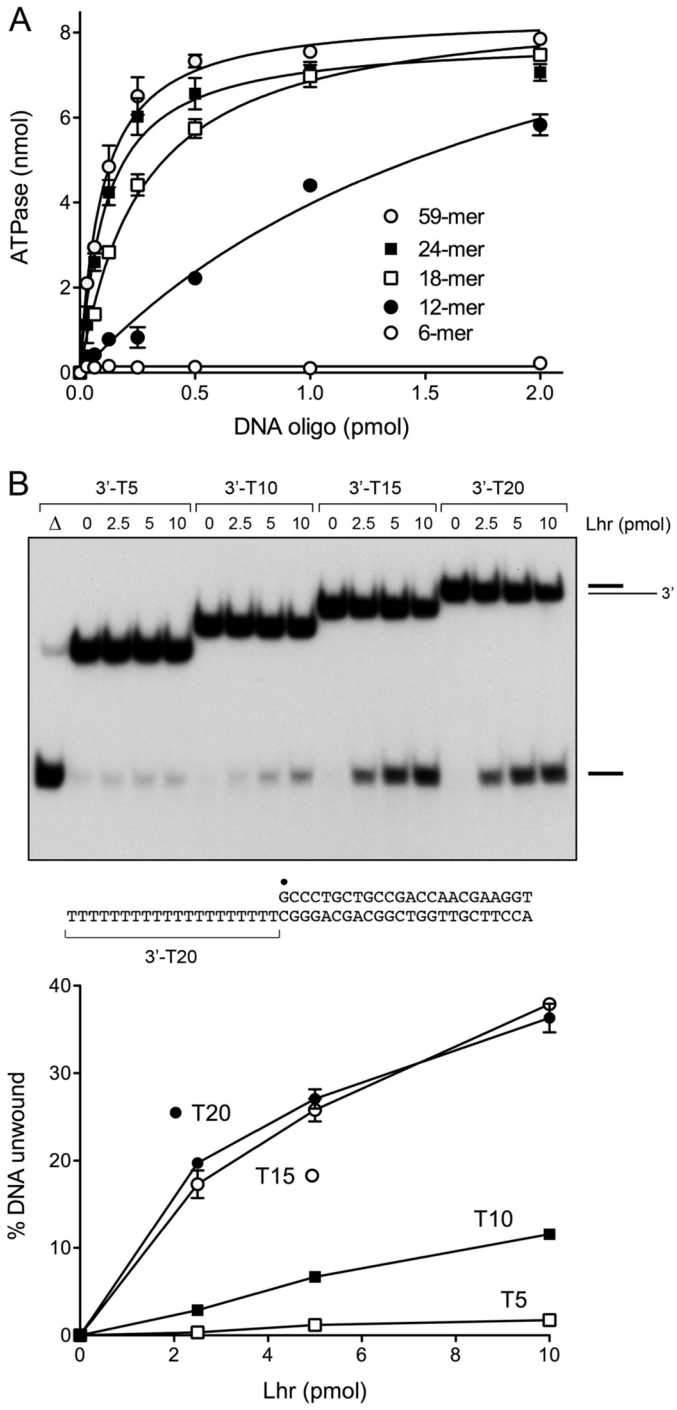

FIGURE 7. **Single strand DNA length requirements for ATPase and helicase activity.** *A*, ATPase reaction mixtures (10 μl) containing 20 mM Tris-HCl, pH 7.0, 1 mM DTT, 1 mM $CaCl_2$, 1 mM [α-^{32}P]ATP, 100 nM Lhr, and increasing amounts of 59-mer, 24-mer, 18-mer, 12-mer, or 6-mer oligodeoxynucleotides as specified were incubated at 37 °C for 30 min. The extents of ATP hydrolysis are plotted as a function of input oligonucleotide (pmol). Data are the average of three separate DNA titration experiments ± S.E. A nonlinear regression curve fit of the data to a one site binding equation (in Prism) is shown. *B*, helicase reaction mixtures (10 μl) contained 20 mM Tris-HCl, pH 7.0, 1 mM DTT, 5 mM $CaCl_2$, 100 nM of the 3′-T5, -T10, -T15, or -T20 tailed duplex DNA substrates (depicted at the *bottom*, with the 5′ ^{32}P label denoted by a *filled circle*), 1 mM ATP, and Lhr as specified. The reaction products were analyzed by native PAGE and visualized by autoradiography. The extents of duplex winding [ssDNA ÷ (ssDNA + tailed duplex DNA)] were quantified by scanning the gel and are plotted as a function of input Lhr in the *bottom panel*. Data are the average of three separate helicase titration experiments ± S.E.

Tail Length Requirement for Duplex DNA Unwinding—To probe the 3′ tail requirement for duplex unwinding by Lhr, we tested a series of helicase substrates with 3′-oligo(dT) tails of varying length (20, 15, 10, or 5 nucleotides) attached to an identical 24-bp duplex segment (Fig. 7*B*). Lhr-mediated displacement of the labeled 24-mer strand was equivalent when the 3′ tail was 15 or 20 nucleotides; helicase specific activity decreased by a factor of six when the 3′ tail was retracted to 10 nucleotides (Fig. 7*B*). Virtually no unwinding was seen when the tail was shortened to only five nucleotides. The loading strand 3′ tail

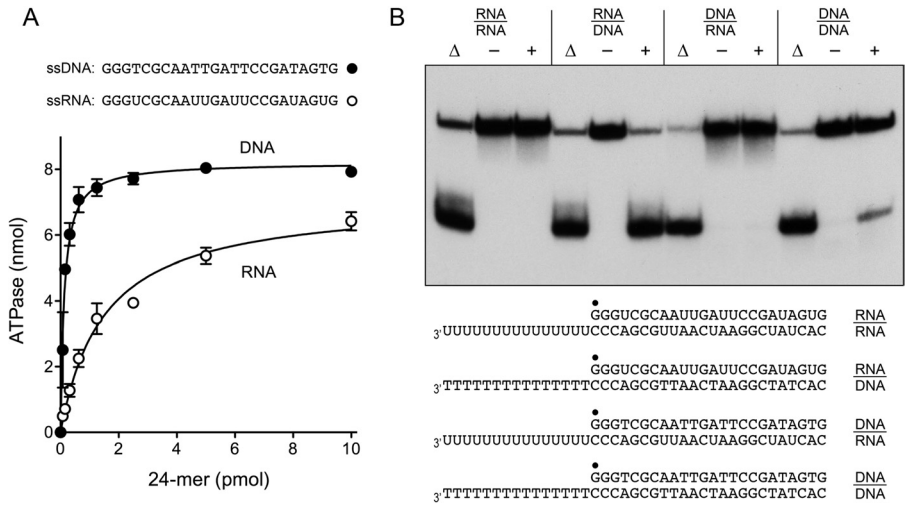

FIGURE 8. **Lhr ATPase and helicase activity with DNA and RNA substrates.** *A*, ATPase reaction mixtures (10 μl) containing 20 mM Tris-HCl, pH 7.0, 1 mM DTT, 1 mM $CaCl_2$, 1 mM [α-^{32}P]ATP, 100 nM Lhr, and the indicated amount of 24-mer DNA or RNA were incubated at 37 °C for 30 min. The sequences of the 24-mer DNA and RNA strands are depicted at the *top*. The extents of ATP hydrolysis are plotted as a function of input 24-mer. Data are the average of three separate nucleic acid titration experiments ± S.E. A nonlinear regression curve fit of the data to a one-site binding equation (in Prism) is shown. *B*, helicase reaction mixtures (10 μl) contained 20 mM Tris-HCl, pH 7.0, 1 mM DTT, 5 mM $CaCl_2$, 50 nM of the indicated DNA:DNA, RNA:RNA, or RNA:DNA hybrid substrates (depicted at the *bottom*, with the 5′ ^{32}P label denoted by *filled circles*), 1 mM ATP, and 250 nM Lhr (+). Enzyme was omitted from the reaction mixtures in lanes (−). A reaction mixture lacking enzyme that was heat denatured prior to PAGE in included in *lane* Δ. The reaction products were analyzed by native PAGE and visualized by autoradiography.

length requirements paralleled the length requirements for activation of the DNA-dependent ATPase (Fig. 7*A*).

Activation of ATP Hydrolysis by RNA—DNA and RNA strands of otherwise identical size (24-mer) and nucleobase sequence (excepting U for T in RNA) were tested as cofactors for the Lhr ATPase. The dependence of ATP hydrolysis on the level of input DNA or RNA is shown in Fig. 8*A*. The apparent K_d values for the 24-mer DNA and RNA, obtained by nonlinear regression curve fitting of the data in Prism, were 13 ± 1.9 nM and 150 ± 20 nM, respectively. (The calculated activity plateau for the RNA-dependent ATPase reaction was ~85% of the DNA-dependent reaction.)

Lhr Unwinds an RNA:DNA Hybrid with DNA as the Loading Strand—The RNA-dependent ATPase activity of Lhr raises the question of whether the motor can unwind RNA-containing duplexes. To address this issue, we prepared a series of helicase substrates, consisting of a 24-bp duplex and a 15-mer 3′ single strand tail, in which the 39-mer loading strand was DNA or RNA of otherwise identical nucleobase sequence (excepting U for T in RNA), and the 24-mer displaced strand was DNA or RNA of identical nucleobase sequence (Fig. 8*B*). The instructive findings from an initial assay of unwinding of 50 nM duplex by 250 nM Lhr were as follows: (i) an RNA:DNA hybrid with a DNA loading strand was a better helicase substrate than a DNA:DNA duplex; (ii) Lhr failed to unwind a 3′-tailed RNA:RNA duplex; and (iii) Lhr did not unwind a DNA:RNA hybrid with a 39-mer RNA loading strand (Fig. 8*B*). Lhr titration experiments showed that the specific activity of the full-length enzyme in unwinding the RNA:DNA hybrid (Fig. 9*B*) was 8-fold greater than its activity in unwinding the DNA:DNA duplex (Fig. 9*A*).

Distinctive Effects of C-terminal Truncations on DNA:DNA Versus RNA:DNA Unwinding—Deletion of the C-terminal 409 or 651 amino acids of Lhr had little impact on the ATPase activity of Lhr (Fig. 2*B*) and did not impair its 3′-to-5′ translocase activity on single strand DNA, as gauged by streptavidin

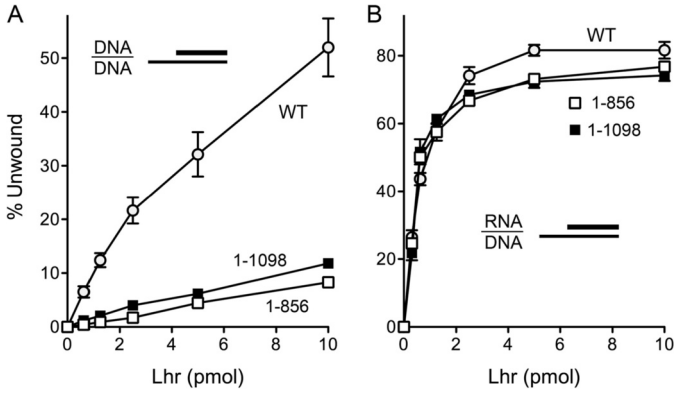

FIGURE 9. **Helicase activity of Lhr truncations on a 3′-tailed DNA:DNA or RNA:DNA duplex substrate.** Helicase reaction mixtures (10 μl) contained 20 mM Tris-HCl, pH 7.0, 1 mM DTT, 5 mM $CaCl_2$, either 50 nM of 5′ ^{32}P-labeled 3′-tailed DNA:DNA duplex substrate (*A*) or RNA:DNA duplex with a 3′-DNA tail (*B*) and the indicated amount of full-length wild-type Lhr, or truncated enzymes Lhr-(1–1098) or Lhr-(1–856). The products were analyzed by native PAGE. The extents of duplex winding [ssDNA ÷ (ssDNA + tailed duplex)] were quantified by scanning the gel and are plotted as a function of input Lhr. Data are the average of three separate helicase titration experiments ± S.E. Specific activities in DNA:DNA unwinding and RNA:DNA unwinding were calculated from the slopes of the titration curves in the linear range of enzyme dependence, as determined by linear regression curve fitting in Prism.

displacement (Fig. 5). By assaying the dependence of ATP hydrolysis on the level of input 24-mer DNA, we found that the apparent K_d values of Lhr-(1–1098), and Lhr-(1–856) for the 24-mer DNA were 12 nM and 10 nM, respectively (data not shown), signifying that the C-terminal deletions did not diminish the affinity of Lhr for the DNA cofactor for ATP hydrolysis. However, when we compared the DNA:DNA unwinding activities of Lhr-(1–1098) and Lhr-(1–856) to that of full-length Lhr, we noted that the C-terminal deletions reduced helicase specific activity to 14 and 9% of the wild-type activity, respectively (Fig. 9*A*). By contrast, the same C-terminal deletions had no impact on the specific activity of Lhr as an RNA:DNA helicase (Fig. 9*B*). These results signify that the C-terminal 409-aa segment enables Lhr to

translocate through a DNA:DNA duplex but is dispensable for its translocation through an RNA:DNA hybrid.

DISCUSSION

The present study unveils mycobacterial Lhr as the founding member of a novel clade of SF2 helicases, by virtue of its distinctive biochemical specificities and its signature domain organization. Lhr is a monomeric nucleic acid-dependent ATPase that uses the energy of nucleotide hydrolysis to drive 3′-to-5′ translocation along single strand DNA and to unwind duplex DNA or an RNA:DNA hybrid *en route*. The ATPase is more active in the presence of calcium than magnesium, a feature that distinguishes Lhr from previously characterized mycobacterial helicases. (To wit, UvrD1 is inactive when magnesium is replaced by calcium (4); RqlH is more active with magnesium than calcium (12); and SftH is equally active with magnesium and calcium (13).) Lhr has no appreciable ATPase activity in the absence of nucleic acid; its phosphohydrolase function is triggered by either single strand DNA or single strand RNA, yet the apparent affinity for the DNA activator is 11-fold higher than for an RNA strand of identical size and nucleobase sequence. The remarkable property of Lhr is that it is 8-fold better at unwinding an RNA:DNA hybrid duplex when translocating on a 3′-tailed DNA loading strand than it is at displacing a DNA:DNA duplex of identical nucleobase sequence. Yet, Lhr is unable to unwind a duplex when the loading strand is RNA.

To score in the single turnover helicase assay, the motor must initiate ATP hydrolysis and directional translocation on the 3′ single strand tail of the loading strand and advance into the duplex segment, prying the strands apart as it moves, to the point that either the non-loading strand is traversed completely and thereby ejected or to a position in the duplex region where the level of residual base pairing is low enough for the strand to dissociate spontaneously. Thus, the inability of Lhr to unwind from an RNA loading strand, despite the efficacy of RNA in activating the ATPase, could signify that ATP hydrolysis is uncoupled, or loosely coupled, to translocation when the effector nucleic acid is RNA (*i.e.* Lhr dissociates more readily from an RNA strand after ATP hydrolysis). More interesting is the fact that an RNA strand is preferred over a DNA strand for displacement when Lhr translocates along a DNA loading strand. Possible explanations for this result are as follows: (i) that Lhr senses the helical conformation of the duplex at its leading edge and prefers the A-form helix of an RNA:DNA hybrid to the B-form DNA:DNA duplex or (ii) that Lhr interacts directly with the displaced non-loading strand and RNA is preferred in this regard.

The ATPase, DNA translocase, and RNA:DNA helicase activities of mycobacterial Lhr are encompassed within an N-terminal 856-aa segment of the 1507-aa polypeptide. This autonomous helicase consists of a classical SF2 (DExH-box) motor domain embraced within the N-terminal ~500 amino acids. However, the Lhr-(1–562) fragment containing the motor domain does not suffice for ATP hydrolysis, signifying that the region from aa 563–856 contributes structural elements necessary for DNA-dependent ATP hydrolysis. The Lhr segment from aa 657 to 847 is classified at NCBI as a "pfam08494" domain. This module, of unknown structure or function, is fused in *cis* to an upstream helicase-like NTPase domain in many biochemically uncharacterized proteins in the NCBI database. Indeed, the abbreviated Lhr-(1–856) helicase enzyme *per se* exemplifies a large family of homologous polypeptides, all of similar size (~800–900 aa), present in the proteomes of scores of diverse bacterial and archaeal taxa. The salient property of the Lhr-(1–856) helicase illuminated presently is that it is 100-fold more active in unwinding the tailed RNA:DNA hybrid substrate than the tailed DNA:DNA duplex (Fig. 9). (We speculate below on the possible role of Lhr or Lhr-(1–856) helicases in the repair of gaps flanking RNA-primed DNAs.)

In our view, the domain organization of full-length mycobacterial Lhr is sufficiently distinctive to warrant the designation of Lhr as the exemplar of a new SF2 helicase clade. A search of the NCBI databases with *M. smegmatis* Lhr recovered scores of bacterial Lhr-like proteins, of similar length (1400 to 1700 aa), and containing a C-terminal segment homologous to the inessential portion of mycobacterial Lhr downstream of aa 856. The C-terminal domain of mycobacterial Lhr (aa 856–1507), although not important for RNA:DNA unwinding, apparently does enable the DNA:DNA helicase activity. We find no functionally instructive motifs within this portion of mycobacterial Lhr. Homologs of full-length Lhr that include the C-terminal domain are found in diverse bacterial taxa from eight different phyla (supplemental Table S1). They are especially prevalent in Actinobacteria (in >50 genera) and Proteobacteria (more than 25 genera) (supplemental Table S1). We did not find "full-length" Lhr homologs in archaea.

Two independent studies of the transcriptional response of *M. tuberculosis* to DNA damaging agents have identified the Rv3296 gene (encoding the Lhr helicase) as being up-regulated in bacteria exposed to UV irradiation or mitomycin C (26, 27). The genes encoding helicases AdnAB (Rv3201c Rv3202c) and UvrD2 (Rv3198c) are also up-regulated in response to DNA damage (26, 27). Such studies implicate Lhr in DNA repair or recombination. Given that Lhr is most adept at translocating 3′-to-5′ after loading on single strand DNA and then displacing an RNA strand annealed to the tracking strand, we speculate that Lhr might participate in the repair of gaps flanking RNA-primed Okazaki fragments, *e.g.* by peeling off the 5′ RNA segments and exposing them to a flap endonuclease-like processing enzyme. This echoes the suggestion by Steven Matson (28) that the *E. coli* 3′-to-5′ helicase UvrD might unwind the RNA component of Okazaki fragments, prompted by his finding that UvrD preferred to unwind RNA:DNA hybrids compared with DNA:DNA hybrids of similar length.

It is unlikely that Lhr activity is necessary for Okazaki fragment maturation under normal growth conditions, insofar as Lamichhane *et al.* (29) have isolated viable strains of *M. tuberculosis* in which the *lhr* gene is disrupted by a transposon inserted at nucleotide positions 631 or 2457 of the 4541-nucleotide *lhr* open reading frame. The proximal transposon insert would ablate all Lhr activities. It is attractive to think that Lhr activity comes into play during conditions of DNA damage or replication fork arrest, in which restart of leading strand synthesis or arrest of the lagging strand polymerase result in gaps between an upstream replicated strand and a downstream RNA-primed strand. Our initial biochemical analysis provides

impetus for future studies, including the following: (i) characterization of the *in vivo* effects of ablating *lhr* in *M. smegmatis*, singly and in combination with other potentially redundant inessential *M. smegmatis* helicase genes (*adnAB*, *uvrD1*, *rqlH*, *recBCD*, *sftH*); and (ii) structural analyses, especially of the distinctive pfam08494 and C-terminal domains.

REFERENCES

1. Singleton, M. R., Dillingham, M. S., and Wigley, D. B. (2007) Structure and mechanism of helicases and nucleic acid translocases. *Annu. Rev. Biochem.* **76,** 23–50
2. Sinha, K. M., Stephanou, N. C., Gao, F., Glickman, M. S., and Shuman, S. (2007) Mycobacterial UvrD1 is a Ku-dependent DNA helicase that plays a role in multiple DNA repair events, including double-strand break repair. *J. Biol. Chem.* **282,** 15114–15125
3. Sinha, K. M., Glickman, M. S., and Shuman, S. (2009) Mutational analysis of Mycobacterium UvrD1 identifies functional groups required for ATP hydrolysis, DNA unwinding, and chemomechanical coupling. *Biochemistry* **48,** 4019–4030
4. Curti, E., Smerdon, S. J., and Davis, E. O. (2007) Characterization of the helicase activity and substrate specificity of *Mycobacterium tuberculosis* UvrD. *J. Bacteriol.* **189,** 1542–1555
5. Güthlein, C., Wanner, R. M., Sander, P., Davis, E. O., Bosshard, M., Jiricny, J., Böttger, E. C., and Springer, B. (2009) Characterization of the mycobacterial NER system reveals novel functions of the *uvrD1* helicase. *J. Bacteriol.* **191,** 555–562
6. Houghton, J., Townsend, C., Williams, A. R., Rodgers, A., Rand, L., Walker, K. B., Böttger, E. C., Springer, B., and Davis, E. O. (2012) Important role for *Mycobacterium tuberculosis* UvrD1 in pathogenesis and persistence apart form its function in nucleotide excision repair. *J. Bacteriol.* **194,** 2916–2923
7. Sinha, K. M., Stephanou, N. C., Unciuleac, M. C., Glickman, M. S., and Shuman, S. (2008) Domain requirements for DNA unwinding by mycobacterial UvrD2, an essential DNA helicase. *Biochemistry* **47,** 9355–9364
8. Williams, A., Güthlein, C., Beresford, N., Böttger, E. C., Springer, B., and Davis, E. O. (2011) UvrD2 is essential in *Mycobacterium tuberculosis*, but its helicase activity is not required. *J. Bacteriol.* **193,** 4487–4494
9. Poterszman, A., Lamour, V., Egly, J. M., Moras, D., Thierry, J. C., and Poch, O. (1997) A eukaryotic XBP/ERCC3-like helicase in *Mycobacterium leprae*? *Trends Biochem. Sci.* **22,** 418–419
10. Biswas, T., Pero, J. M., Joseph, C. G., and Tsodikov, O. V. (2009) DNA-dependent ATPase activity of bacterial XBP helicases. *Biochemistry* **48,** 2839–2848
11. Balasingham, S. V., Zegeye, E. D., Homberset, H., Rossi, M. L., Laerdahl, J. K., Bohr, V. A., and Tønjum, T. (2012) Enzymatic activities and DNA substrate specificity of *Mycobacterium tuberculosis* DNA helicase XPB. *PLoS One* **7,** e36960
12. Ordonez, H., Unciuleac, M., and Shuman, S. (2012) Mycobacterium smegmatis RqlH defines a novel clade of bacterial RecQ-like DNA helicases with ATP-dependent 3′-5′ translocase and duplex unwinding activities. *Nucleic Acids Res.* **40,** 4604–4614
13. Yakovleva, L., and Shuman, S. (2012) Mycobacterium smegmatis SftH exemplifies a distinctive clade of superfamily II DNA-dependent ATPases with 3′ to 5′ translocase and helicase activities. *Nucleic Acids Res.* **40,** 7465–7475
14. Zegeye, E. D., Balasingham, S. V., Laerdahl, J. K., Homberset, H., and Tønjum, T. (2012) *Mycobacterium tuberculosis* RecG binds and unwinds model DNA substrates with a preference for Holliday junctions. *Microbiology* **158,** 1982–1993
15. Sinha, K. M., Unciuleac, M. C., Glickman, M. S., and Shuman, S. (2009) AdnAB: a new DSB-resecting motor-nuclease from Mycobacteria. *Genes Dev.* **23,** 1423–1437
16. Unciuleac, M. C., and Shuman, S. (2010) Characterization of the mycobacterial AdnAB DNA motor provides insights to the evolution of bacterial motor-nuclease machines. *J. Biol. Chem.* **285,** 2632–2641
17. Unciuleac, M. C., and Shuman, S. (2010) Double-strand break unwinding and resection by the mycobacterial helicase-nuclease AdnAB in the presence of mycobacterial SSB. *J. Biol. Chem.* **285,** 34319–34329
18. Gupta, R., Barkan, D., Redelman-Sidi, G., Shuman, S., and Glickman, M. S. (2011) Mycobacteria exploit three genetically distinct DNA double-strand break repair pathways. *Mol. Microbiol.* **79,** 316–330
19. Reuven, N. B., Koonin, E. V., Rudd, K. E., and Deutscher, M. P. (1995) The gene for the longest known *Escherichia coli* protein is a member of helicase superfamily II. *J. Bacteriol.* **177,** 5393–5400
20. Bernstein, D. A., Zittel, M. C., and Keck, J. L. (2003) High-resolution structure of the *E. coli* RecQ helicase core. *EMBO J.* **22,** 4910–4921
21. Gu, M., and Rice, C. M. (2010) Three conformational snapshots of the hepatitis C virus NS3 helicase reveal a ratchet translocation mechanism. *Proc. Natl. Acad. Sci. U.S.A.* **107,** 521–528
22. Olsen, I., Balasingham, S. V., Davidsen, T., Debebe, E., Rødland, E. A., van Soolingen, D., Kremer, K., Alseth, I., and Tønjum, T. (2009) Characterization of the major formamidopyrimidine-DNA glycosylase homolog in *Mycobacterium tuberculosis* and its linkage to variable tandem repeats. *FEMS Immunol. Med. Microbiol.* **56,** 151–161
23. Morris, P. D., and Raney, K. D. (1999) DNA helicases displace streptavidin from biotin-labeled oligonucleotides. *Biochemistry* **38,** 5164–5171
24. Morris, P. D., Byrd, A. K., Tackett, A. J., Cameron, C. E., Tanega, P., Ott, R., Fanning, E., and Raney, K. D. (2002) Hepatitis C virus NS3 and simian virus 40 T antigen helicases displace streptavidin from 5′-biotinylated oligonucleotides but not from 3′-biotinylated oligonucleotides: evidence for directional bias in translocation on single-stranded DNA. *Biochemistry* **41,** 2372–2378
25. Byrd, A. K., and Raney, K. D. (2004) Protein displacement by an assembly of helicase molecules aligned along single-stranded DNA. *Nat. Struct. Mol. Biol.* **11,** 531–538
26. Rand, L., Hinds, J., Springer, B., Sander, P., Buxton, R. S., and Davis, E. O. (2003) The majority of inducible DNA repair genes in *Mycobacterium tuberculosis* are induced independently of RecA. *Mol. Microbiol.* **50,** 1031–1042
27. Boshoff, H. I., Reed, M. B., Barry, C. E., 3rd, and Mizrahi, V. (2003) DnaE2 polymerase contributes to *in vivo* survival and the emergence of drug resistance in *Mycobacterium tuberculosis*. *Cell* **113,** 183–193
28. Matson, S. W. (1989) *Escherichia coli* DNA helicase II (*uvrD* gene product) catalyzes the unwinding of DNA·RNA hybrids *in vitro*. *Proc. Natl. Acad. Sci. U.S.A.* **86,** 4430–4434
29. Lamichhane, G., Zignol, M., Blades, N. J., Geiman, D. E., Dougherty, A., Grosset, J., Broman, K. W., and Bishai, W. R. (2003) A postgenomic method for predicting essential genes at subsaturation levels of mutagenesis: application to *Mycobacterium tuberculosis*. *Proc. Natl. Acad. Sci. U.S.A.* **100,** 7213–7218